J Therm Anal Calorim (2012) 108:109–117
DOI 10.1007/s10973-011-1695-2

Kinetic study of decomposition of wheat distiller grains and steam gasification of the corresponding pyrolysis char

Guiying Xu · Baizeng Fang · Guogang Sun

Received: 31 March 2011 / Accepted: 24 May 2011 / Published online: 26 June 2011

Abstract Thermal characteristics of wheat distiller grains (WDGs) and steam gasification kinetics of the corresponding pyrolysis char were studied by thermogravimetric analysis. The pyrolysis process of WDGs can be divided into three stages including the drying, devolatilization, and carbonation. The heating rate and final temperature are the most important factors influencing the WDGs decomposition. The ultimate mass loss increases with increasing final temperature while the mass loss rate and the characteristic temperature for the maximum reaction rate increase with the increasing heating rate. For the pyrolysis of WDGs, the average activation energy was calculated as 77.45 kJ mol^{-1} by Coats–Refern method. While for the steam gasification of the pyrolysis char, the shrinking-core model fits the gasification behavior better than the volumetric reaction one and the activation energy, and the pre-exponential factor were calculated to be 199.19 kJ mol^{-1} and 7.21 $\times$ 10^6 s^{-1}, respectively, with the former model.

Keywords Distiller grains · Pyrolysis char · Steam gasification · Kinetics · Thermal analysis

G. Xu (✉) · G. Sun (✉)
Laboratory of Heavy Oil Processing, China University of Petroleum-Beijing, Beijing 102249, China
e-mail: xgy092500@126.com

G. Sun
e-mail: ggsunbj@126.com

B. Fang
Chemical and Biological Engineering, University of British Columbia, Vancouver, BC V6T 1Z4, Canada

Introduction

With the depletion of fossil fuel sources as well as the global warming issues, considerable attention has been focused on the development of alternative fuels [1]. Biomasses are known to grow in a sustained way through the fixation and release of CO_2, mitigating global warming problems [2, 3]. At present, thermochemical conversion of biomass by pyrolysis, gasification, and combustion is becoming increasingly important for the efficient production of fuels in commercial and industrial applications for power generation in diesels or boilers [4–6]. Distillers grains (DGs) are a cereal byproduct of the distillation process. It has been estimated that the world produces as much as 60 million tonnes of dry distillers grains (DDGs) each year [7]. Large amount of DGs has been concentrated in distiller plant in every country, which can pollute the environment if not treated promptly, and the heat value of rotten biomass will decrease a lot. Previously, DGs were thrown away as waste, and later mainly used for animal feed [8–10]. Because DGs contain alcohol content and a large number of bacteria, a long-term consumption of DGs by livestock may cause the animals to experience toxic reactions, which can finally affect the health of consumers. In addition, transportation of DDGs to distant locations for utilization is expensive [11]. Thus, conversion of DDGs to chemical energy in the plant sites seems to be logically viable for utilizing these waste biomasses. At present, DGs are used for anaerobic digestion for producing biogas [12, 13], which has a main drawback, namely, that less than 60% volatile matter is utilized, forming high water content residue including other volatile matter, fixed carbon, and ash. The issue of how to deal with these residues is a new problem, and the construction and operating costs are high. Therefore, the efficient use of DGs is of great

significance for development of resources and environmental protection.

DGs are rich in protein and fat content, which is a potential feedstock for thermochemical conversion. At present, some researchers study the gasification characteristics of DGs. Tavasoli et al. [11] studied production of hydrogen and syngas via gasification of the corn and wheat DDGs with oxygen in a continuous downflow fixed bed micro-reactor. Gasification of corn DDGs demonstrated a higher gas yield (i.e., 0.42 m^3/kg), lower heating value (LHV) (10.65 MJ m^{-3}) and carbon conversion efficiency (44.2%), slightly higher than those from gasification of wheat DDGs. Kumar et al. [14] investigated gasification of DDGs on a bench-scale fluidized-bed gasifier with steam and air as fluidizing and oxidizing agents. The carbon conversion efficiency was reported to be above 95% by choosing proper operating conditions. Thus, thermochemical utilization of DGs will not only provide rational use of organic contents of DGs, but also can handle the waste effectively. Unfortunately, so far there has not been any report about the design of reactors for efficient thermochemical conversion of wheat DGs (WDGs). Pyrolysis is the first chemical step in gasification, and the conversion of char occurs at higher temperatures when most of thermal decomposition processes are finished [15]. To carry out an ideal design of the systems for thermochemical treatment and proper control of WDGs, it is necessary to study the pyrolysis processes of WDG and, steam gasification of the corresponding pyrolysis char, and to determine the kinetic parameters which can provide basic data for the design of the gasification reactor of WDGs.

Experimental

Materials

WDGs

WDGs were obtained from Jilin Brewery, being located in Baishan city (China). To ensure the uniformity of the temperature in the sample, the size of WDGs is recommended to be small [16, 17]. Grains were ground and sieved, and the fraction of 60–90 μm in particle size was used for the experimental runs. The proximate and ultimate analyses of WDGs are given in Table 1.

Biomass char

The amount of char produced by TG was not enough for ultimate and specific surface area analyses, and so a tube furnace (model SK2-2-10H) was used to produce the char at the same preparation conditions of TG for the ultimate analysis and specific surface area analyses. The tube furnace consists of a quartz tube with a diameter of 50 mm, a heating furnace, and two end caps. The temperature can be controlled to within ±5 °C. 8 g of WDGs was used in every run. Nitrogen with a flow rate of 100 ml/min was introduced into the furnace at the heating rate of 20 K/min. The final temperature, 1000 °C, was maintained for 30 min to degas the char. The analysis results are shown in Table 2.

Experimental process

Decomposition process under nitrogen atmosphere

A Shimadzu DTG60 TG analyzer was used to measure the change of sample mass with temperature during the reaction. The most common range of ramp heating rate reported by the literature for TG characterization of biomass was 5–50 K/min [18–23], and thus TG curves were obtained at three different heating rates (i.e., 10, 20, and 30 K/min) between the room temperature and 923 K for the pyrolysis. The precision of the reported temperatures was estimated to be ±2 °C. Nitrogen, an inert purge gas, was introduced into the furnace with a flow rate of 50 ml/min. Before starting each pyrolysis experiment, nitrogen was fed into the furnace for 40 min to eliminate the residual air in the pyrolysis zone, thereby avoiding unwanted oxidation of the sample. The thermal balance recorded the mass signals automatically during experiments, and all the data were analyzed using origin 8.0. The temperature and mass signals were calibrated before each test. The reproducibility of the experiments was acceptable, and the experimental data presented in this article corresponding to the different operating conditions represented the mean values of runs conducted two or three times. All the sample amounts used in this study averaged approximately 10 mg to exclude the effects of diffusion.

Table 1 Characteristics of the experimental materials: proximate and elemental analysis of WDGs

Material	Proximate analysis/%				Ultimate analysis/%					Q/MJ kg^{-1}
	V_{ad}	FC_{ad}	A_{ad}	M_{ad}	C_d	H_d	O_{cad}	N_d	$S_{t,d}$	
Wheat DGs	77.01	13.64	2.35	7.00	39.03	5.16	28.36	1.63	0.17	12.86

Table 2 Characteristics of the experimental materials: characteristics of the biomass char prepared at 1000 °C

Material	Ultimate analysis/%						Specific surface area/m^2/g
	C_d	H_d	Ash	O_{cad}	N_d	S_d	
Char	59.98	<0.3	26.04	13.38	0.96	<0.3	415.81

Steam gasification process

Biomass was placed on a shallow alumina pan (<1 mm in the depth), heated to 1000 °C at a heating rate of 20 K/min under nitrogen atmosphere. Nitrogen was introduced into the furnace with a flow rate of 50 ml/min during the pyrolysis process. After the furnace was kept at 1000 °C for 30 min, the distilled water was injected into the furnace controlled by a syringe pump. The nitrogen flow rate was changed to 200 ml/min during the steam gasification process automatically. The steam partial pressure values are accurate within ±3.0% considering the accuracies of the water pump and the TG mass flow controller. Steam was mixed with nitrogen in the furnace to react with the char which was produced by the pyrolysis process in the furnace of TG. The reaction time is controlled by the gasification temperature. To decrease the effects of diffusion between the char sample and the gas phase, a small particle size in range of 0–40 μm was used in the experiments.

Theory applied to determine kinetics parameters

The kinetic analysis of solid–state decomposition is usually based on a single-step kinetic equation:

$$\frac{d\alpha}{dt} = k(T)f(\alpha) \tag{1}$$

$$\alpha = \frac{m_0 - m_t}{m_0 - m_f} \tag{2}$$

where α is the extent of conversion; t is the reaction time; T is the temperature of the reaction, k (T) is a function of T, and f (α) is the reaction model which represents the reaction mechanism, also a function of α.

In the late nineteenth century, Arrhenius and Van't proposed K–T equation [24]:

$$k(T) = A\exp\left(-\frac{E}{RT}\right) \tag{3}$$

where A and E are the Arrhenius parameters, pre-exponential factor and activation energy, respectively; and R is Prandtl gas constant, 8.314 J (mol k).

Equations 1 and 3 can be combined to obtain

$$\frac{d\alpha}{dt} = A\exp\left(-\frac{E}{RT}\right)f(\alpha) \tag{4}$$

In conditions of linear heating

$$T = T_0 + \beta t \tag{5}$$

Equations 4 and 5 can be combined to obtain

$$\frac{d\alpha}{dT} = \frac{1}{\beta}A\exp\left(-\frac{E}{RT}\right)f(\alpha) \tag{6}$$

Equation 6 can be rearranged as

$$\frac{d\alpha}{f(\alpha)} = \frac{1}{\beta}A\exp\left(-\frac{E}{RT}\right)dT \tag{7}$$

Integrating up to conversion, α, Eq. 7 gives

$$\int_0^{\alpha}\frac{d\alpha}{f(\alpha)} = G(\alpha) = \frac{A}{\beta}\int_{T_0}^{T}\exp\left(-\frac{E}{RT}\right)dT \tag{8}$$

The subscript 0 represents the initial value, and $G(\alpha)$ is the integral of $f(\alpha)$; In general, A, E, and $f(\alpha)$ are called the three factors of kinetics, which are necessary to define the kinetics of a reaction.

Method for decomposition kinetics

In this article, Coats–Refern method [25] was employed to analyze the data of decomposition process of WDGs.

$$\ln\left[\frac{G(\alpha)}{T^2}\right] = \ln\left[\frac{AR}{\beta E}\left(1-\frac{2RT}{E}\right)\right] - \frac{E}{RT} \tag{9}$$

Assuming

$$f(\alpha) = (1-\alpha)^n, \tag{10}$$

$$G(\alpha) = \frac{1-(1-\alpha)^{1-n}}{1-n} \tag{11}$$

For the ordinary reaction temperature and most values of E, $E/RT \gg 1$

$$\ln\left[\frac{AR}{\beta E}\left(1-\frac{2RT}{E}\right)\right] = \cos\tan t \tag{12}$$

$$\ln\left[\frac{G(\alpha)}{T^2}\right] = Y \tag{13}$$

$$\frac{1000}{T} = X \tag{14}$$

Based on the linear relationship between Y and X, the value of E and A can be obtained from the slope and intercept.

Methods for steam gasification

(1) *Volumetric-reaction model* [26]

This model assumes uniform gas diffusion in the entire particles.

$$\frac{dx}{dt} = k_v\,(1-x) \tag{15}$$

where k_v represents the gas constant in volumetric model, and $x = \alpha$, meaning conversion. The model gives conversion-time equation as follows:

$$-\ln(1-x) = k_v t \tag{16}$$

(2) *Shrinking core model* [27]

$$\frac{dx}{dt} = k_G\,(1-x)^{\frac{2}{3}} \tag{17}$$

where k_G represents the gas constant in shrinking core model. The model gives the following conversion-time equation:

$$3[1-(1-x)^{\frac{1}{3}}] = k_G t \tag{18}$$

Results and discussion

Decomposition process

Effect of heating rate on thermal decomposition process under nitrogen atmosphere

Figure 1a, b present typical mass loss and mass loss rate plots, respectively, obtained from the pyrolysis of WDGs at different heating rates (10, 20, and 30 K min^{-1}) from room temperature to 923 K. From the thermal decomposition curves, the pyrolysis process exhibits three mass-loss regions occurring at temperature ranges of 293–530, 530–743, and 743–923 K, corresponding to the drying stage, the devolatilization stage, and the carbonation stage, respectively. In the first stage (i.e., drying stage), the mass loss is about 12%, and there is one peak observed before 530 K from the DTG curves shown in Fig. 1b. Because the WDGs are the residues obtained after brewing, it contains the alcohol content and moisture, and the peak is attributable to the alcohol and water evaporating. During the heating process, the water content decreases with the increasing temperature, and a complete drying stage is reached at about 530 K. The second stage (i.e., the devolatilization stage) is the key stage of the pyrolysis process. The majority of the sample mass loss occurs in this region, and the mass loss reaches up to 60 wt% or more. The final

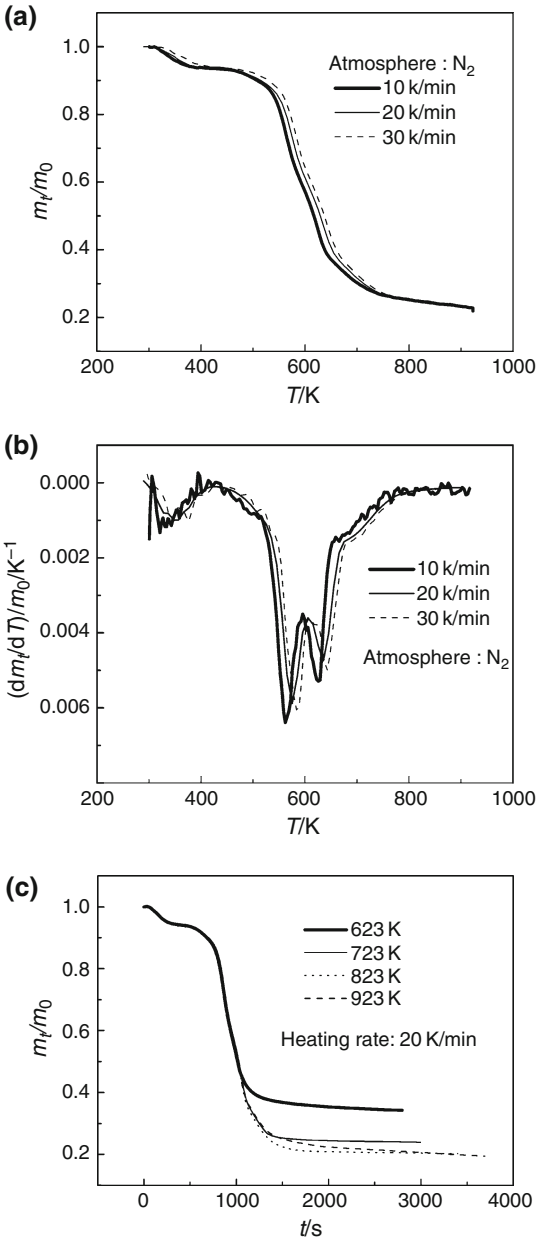

Fig. 1 Thermal decomposition processes for the pyrolysis of WDGs (**a** TG curves,**b** DTG curves, **c** The ultimate mass loss shown against the varying final temperatures)

mass loss at higher heating rates is lower than that at lower heating rates at the same temperature during the second stage. The reaction time is shorter as the heating rate increases, which is unfavorable to promote secondary reactions among tar, char, water, and the produced gas. At this stage, two obvious peaks appear in the DTG curves as shown in Fig. 1b. The temperature parameters derived from the TG and DTG curves are summarized in Table 3. A slow decay in mass loss and a small change in the differential values are observed at the third stage (i.e., the

Table 3 Characteristic devolatilisation temperatures and the corresponding mass loss rate for WDGs

Heating rate K/min	$T1$max/K	$T2$max/K	$T0$/K	Mass loss $T1$max − $T2$max/%	Mass loss at main stage/%	Residue char/%	Mass loss rate at $T1$max/K^{-1}	Mass loss rate at $T2$max/K^{-1}
10	562.41	625.84	525.77	29.33	61.25	21.89	0.00639	0.00529
20	575.55	635.46	535.58	26.12	61.21	22.78	0.00588	0.00474
30	583.58	642.59	548.31	26.03	61.07	22.49	0.00605	0.00499

carbonation stage), which are attributable to the slow decomposition of the residues and the generation of char in the last stage, yielding about 20 wt% of fixed carbon.

Shafizadeh [28] report that the three major constituents of lignocellulosic materials (i.e., hemicellulose, cellulose, and lignin) are chemically reactive, and decompose thermochemically in the temperature range of 423–773 K, (i.e., hemicellulose occurs at 423–623 K, cellulose at 558–623 K, and Lignin at 523–773 K). Thus, decomposition of hemicellulose starts first, followed by the cellulose and the lignin. A temperature level higher than 773 K (i.e., 923 K) was hence selected to compare the residual mass of different straw samples in this study. It can also be seen that the shape of the mass curves does not change with the variation in the heating rate, but the mass loss temperatures show an increase with increasing heating rates, which indicates that the heating rate has a significant influence on the thermal degradation characteristics of biomass components. Other authors [29–31] have also reported that the rates of degradation of various biofuels markedly increased with the increase in the heating rate.

Table 3 lists the temperatures for the start (T_0) of the main mass loss, and the temperatures for the maximum rate of mass loss derived from the two main peaks of the DTG curves at all the applied heating rates. For a TG curve, it is obviously observed that the mass loss starts at low temperature, however, which is not really the decomposition temperature of sludge. It is found that with the increase in the heating rate, the initial degradation temperature increases, which is consistent with that observed by other authors for other biomasses including olive, forest residue, cotton residue, and wood [32, 33]. It is also noticed that there is a lateral shift to higher temperatures in T_1max and T_2max for the DGs as the heating rate is increased. The lateral shift is also illustrated in Fig. 1a, b and has been reported for different types of biomass [34, 35], which is attributable to the delayed decomposition caused by the combined effects of the heat transfer at different heating rates and the kinetics of the decomposition.

Effect of final pyrolysis temperature on mass loss

It is well known that the final temperature is a key factor which has influences on the course and product yield during pyrolysis of a biomass. To investigate these effects, the experiments were carried out at a heating rate of 20 K/min, but with different final temperatures, namely, 623, 723, 823, and 923 K. After the temperature reached the final one, the sample was kept in the furnace for 30 min. Figure 1c shows the variation of the ultimate mass loss with the varying final temperatures, from which it is evident that the ultimate mass loss increases, with the increasing final temperature, from 65.74 wt% to more than 80.60 wt% as the final temperature increases from 623 to 923 K. This trend is due essentially to the increase of the degradation temperature, so that the formation of primary char is successively less approved, compared to volatile formation. The additional mass loss observed during the holding time leads to a only few percentages of the total mass loss, which supports the theory of rapid beginning decomposition followed by very slow degasification of the char. This can be easily understood because the pyrolysis of biomass is the cleavage of different chemical bonds with different strengths which occurred in series during heating. Since the mass loss measured by TG is primarily caused by the tar formation, it was found that tar formation completed at about 873 K [36], after which degasification reactions contribute insignificantly to the total mass loss. Another possibility could be the cracking and secondary reactions occurring in the high-temperature stage when the volatiles leave from the surface of the hot char, hereby reducing the total mass loss. It is evident that the final temperature is a key factor which influences the total volatile matter release. In addition, it was found that the char yield decreases with the increasing final temperature as shown in Table 4. The holding time, after the temperature has reached the final temperature, cannot cause significant mass loss during the

Table 4 Char yield shown as a function of time: at different final pyrolysis temperatures

T_{final}/K	623	723	823	923
Char yield/%	34.26	23.93	20.26	19.40

Table 5 Char yield shown as a function of time: at the heating rate of 20 K/min

Holding time/min	0	10	30
Char yield/%	22.78	21.90	20.69

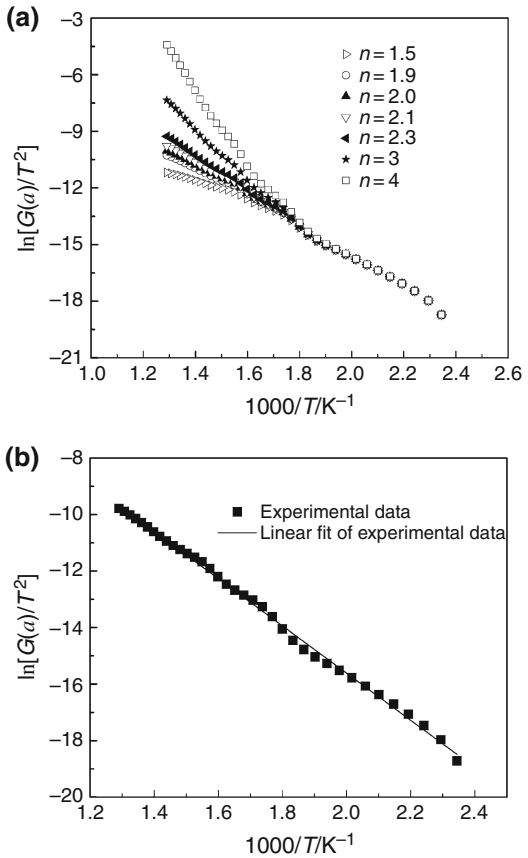

Fig. 2 ln[ln($G(\alpha)/T^2$)] against 1000/T (**a** For different n values; **b** For $n = 2.1$)

pyrolysis. From Table 5, it can be seen that the char yield decreased by 9.17% as the holding time increases from 0 to 30 min at a heating rate of 20 K/min.

Pyrolysis kinetics parameters of WDGs

Coats–Refern single heating rate curve method was employed for the decomposition data analysis in this study, and the least squares fitting method to the analyze TG curves at various heating rates.

$$S = \sum_{i=1}^{i=n} \delta_i^2 = \sum_{i=1}^{i=n} [y_i - \varphi(x_i)]^2 = \min_{\varphi \in H} \sum_{i=1}^{i=n} [y_i - \varphi(x_i)]^2 \quad (19)$$

where (x_i, y_i) forms the experimental data, and $\varphi(x)$ is the demand function. H is a given function category, and a straight line here. We shall try to fit Y and X using different n values till a function of Y and X approaches a straight line. Figure 2a, b show the plots of ln[ln($G(\alpha)/T^2$] against 1000/T for different n values based on the pyrolysis experimental data at the heating rate of 20 K/min. The function of Y and X approaches a straight line as $n = 2.1$. Table 6 summarizes the kinetic parameters for the thermal degradation of WDGs under nitrogen and oxidative atmospheres. The values of n shown in this table are the best fit values having the highest correlation coefficient, R^2 using Coats-refern method. The activation energies and the pre-exponential factors are in the ranges of 70–85 kJ/mol and 5×10^5 to 8×10^6 min^{-1}, respectively.

Table 6 Kinetic parameters of thermal degradation of WDGs under nitrogen atmospheres

		Parameters	Heating rate/K min^{-1}		
			10.0	20.0	30.0
N_2	Main stage	E/kJ/mol	83.68	69.30	79.36
		n	2.7	2.1	3.0
		A	8.14×10^6	4.92×10^5	4.1×10^6
		R^2	0.9916	0.9972	0.9829

Steam gasification process

In this study, the char reactivity was defined as Eq. 15, and the entire steam gasification of chars was evaluated by Eq. 15. Figure 3 shows a typical mass loss curve. The temperature was heated to 1000 °C which was maintained for gasification. The weigh loss curve from c to a represents the pyrolysis process under nitrogen atmosphere, and the curve from a to b represents the steam gasification of the corresponding to pyrolysis of char. The steam pressure has been kept constant ($P_{steam} = 10$ kPa).

$$r(x) = \frac{dx}{(1-x)dt} \quad (20)$$

Effect of reaction temperature

Figure 4a shows the effect of reaction temperature on the fixed carbon conversion. It can be seen that the conversion

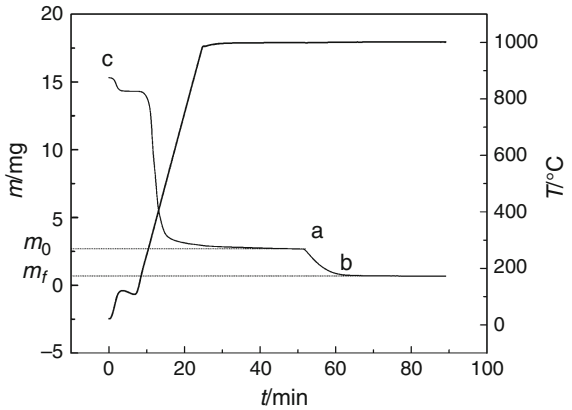

Fig. 3 Typical mass loss during pyrolysis and gasification experiment using TG (WDGs char, 1000 °C, 10 kPa steam)

increases with the increasing time, and high reaction temperature brings about higher conversion at the same reaction time. Figure 4b shows effect of reaction temperature on the char reactivity at $X = 0.5$. It is seen that the char reactivity increases with the increasing temperature. Steam gasification is endothermic reaction, and so increasing the reaction temperature is helpful for promoting the reaction with steam. Figure 5 shows the char reactivity with the function of conversion. It is evident that the reactivity increases as the conversion increases from 0 to 0.6, while it decreases as the conversion increases from 0.6 to 0.9. In a heterogonous reaction, the reactive surface is the key parameter that controls the kinetic. At lower conversion, as carbon conversion increases, many of the pore structure of semi-coke particles will be enlarged by the reaction with steam, and so the reactivity increases with increasing conversion.

Reaction kinetics

To achieve the better kinetic parameters, two models (i.e., volumetric-reaction and shrinking-core models) proposed in the literature were employed here. In order to testify the two models, the linearity was checked based on each model. The relationship between [–ln (1–x)] and time based on volumetric-reaction model and the relationship between [1−(1–x) ^ (1/3)] and time based on shrinking-core model are shown in Fig. 6a, b, respectively. The model equation can be changed into a linear form, so that the value of R^2 stands for the fitting extent of the model to the reaction behavior. The fact that the value of R^2 is close to 1 implies the better fitness of the model to the reaction behavior, while the contrary testifies the invalid model. The plots of

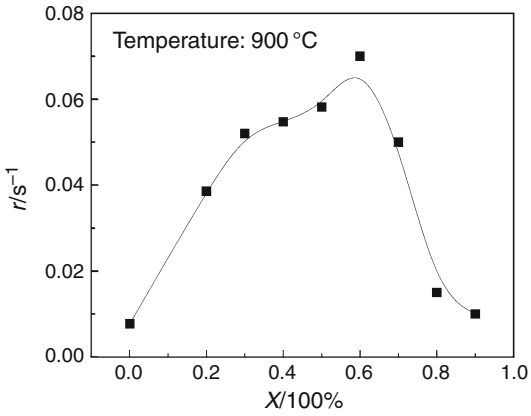

Fig. 5 The char reactivity with the function of conversion

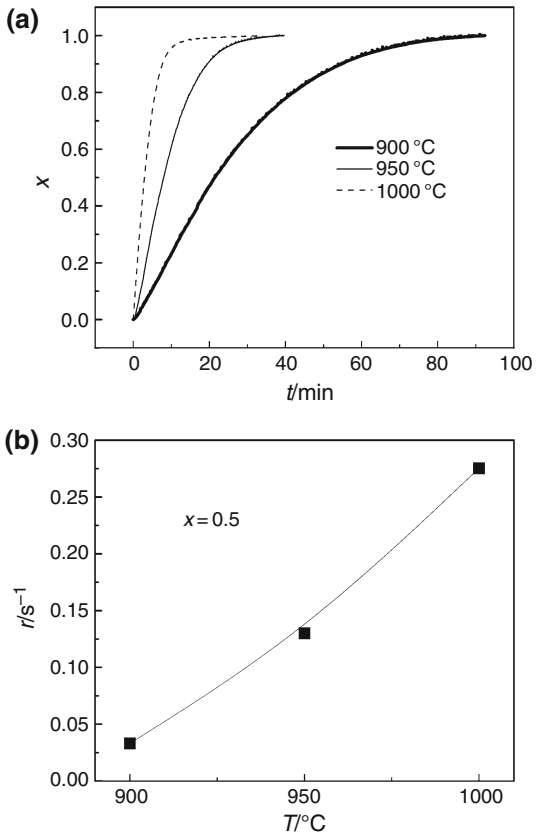

Fig. 4 Effect of reaction temperature (**a** Conversion; **b** The char reactivity when $X = 0.5$)

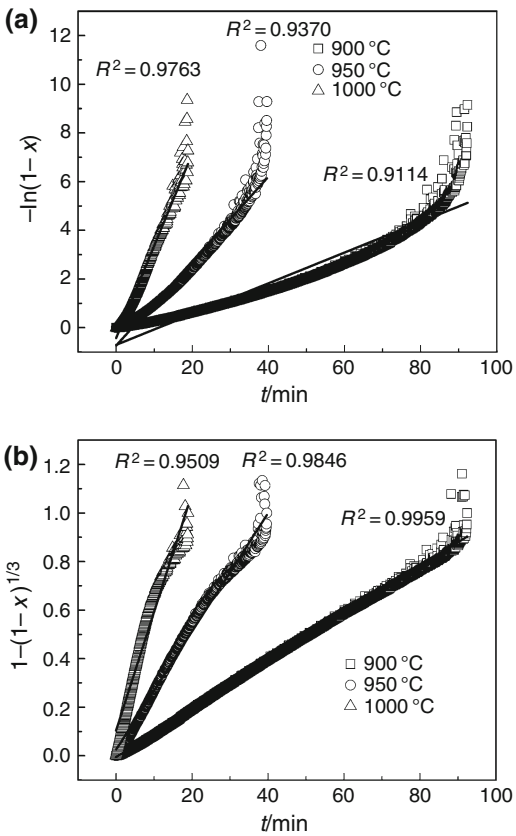

Fig. 6 Conversion function against time (**a** Volumetric-reaction model; **b** Shrinking core model)

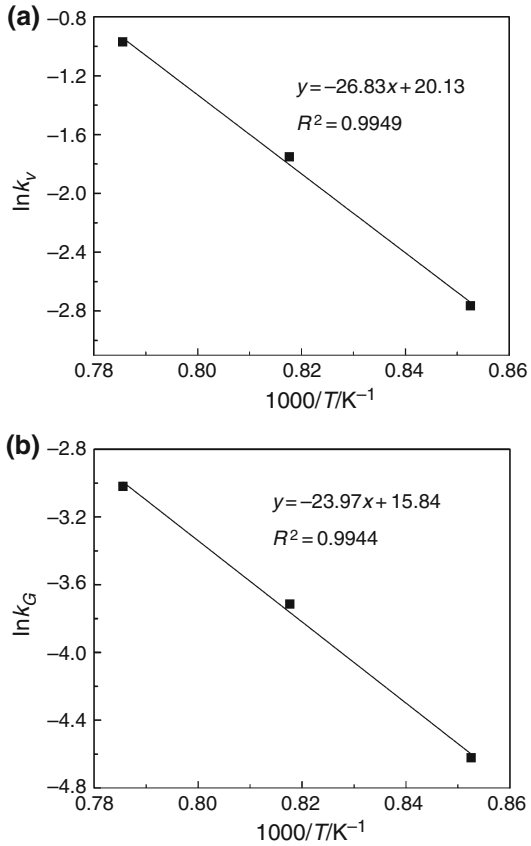

Fig. 7 Arrhenius plot of steam gasification (**a** Volumetric-reaction model; **b** Shrinking core model)

Table 7 The kinetic parameters derived from the various models (Steam pressure = 10 kPa)

Model	*E*/KJ/mol	K_0/s^{-1}
Volumetric-reaction	222.96	5.20×10^8
Shrinking core	199.19	7.21×10^6

Fig. 6a, b reveal that both the two models fit the experimental data well. It can be concluded that the reaction mechanism is chemically controlled for three reaction temperatures (i.e., 900, 950, and 1000 °C). For steam gasification, the reaction temperature is often controlled below 1000 °C [37–39], and so it is unnecessary to investigate the effect of temperature above 1000 °C. The value of R^2 for the volumetric-reaction model is ~0.9366, and it is 0.9771 for the shrinking-core model, which is slightly better than that of the volumetric reaction model. Therefore, it can be said that shrinking-core model better fits the gasification data in the present study. Figure 7a, b represent the Arrhenius plots based on volumetric-reaction and shrinking core models, respectively. From the slope of Arrhenius plot, the activity energy can be obtained. Table 7 shows that the activity energy of the volumetric-reaction model was 222.96 kJ/mol, and that of the shrinking-core model 199.19 kJ/mol. In addition, the pre-exponential factor was 5.20×10^8 s^{-1} by the volumetric-reaction model and 7.21×10^6 s^{-1} by the shrinking-core model over the temperature range 900–1000 °C at a steam pressure of 10 kPa.

Conclusions

In this study, TG was utilized to examine the thermal characteristics at heating rates of 10, 20, and 30 K min^{-1} and the steam gasification kinetics of the corresponding pyrolysis char in temperature range of 900–1000 °C of WDGs. Coats–Redfern method was employed to study the kinetics of the thermal degradation under N_2 at three different heating rates, and the volumetric-reaction and the shrinking-core models were utilized to study pyrolysis char steam gasification. Some typical kinetic parameters such as activation energies, pre-exponential factors, and reaction orders were derived from the experimental data. The average activation energy revealed by Coats–Redfern method for the pyrolysis of WDGs is 77.45 kJ/mol. While for the steam gasification kinetics of the corresponding pyrolysis char, both the volumetric reaction model and the shrinking-core models fit the steam gasification data well, the shrinking-core model fits the gasification behavior better in the present study. The activation energy was 222.96 kJ/mol and the pre-exponential factor was 5.20×10^8 s^{-1} by the volumetric-reaction model, whereas the activation energy was 199.19 kJ/mol and the pre-exponential factor was 7.21×10^6 s^{-1} by the shrinking-core model over the temperature range 900–1000 °C at a steam pressure of 10 kPa. All these kinetics parameters are expected to help one understand better the thermochemical behaviors of the WDGs and design gasification reactors for achieving more efficient thermochemical utilization of the DGs.

Acknowledgements This study was funded by the National Natural Research Program of China(Program no. 20776158)

References

1. Li CS, Suzuki K. Kinetic analyses of biomass tar pyrolysis using the distributed activation energy model by TG/DTA technique. J Therm Anal Calorim. 2009;98:261–6.
2. Mothé CG, De Miranda IC. Characterization of sugarcane and coconut fibers by thermal analysis and FTIR. J Therm Anal Calorim. 2009;97:661–5.
3. Nakanishi M, Ogi T, Fukuda Y. Thermogravimetric analysis in steam and oxygen with gas chromatograph mass spectrometry for basic study of biomass gasification. J Therm Anal Calorim. 2010;101:391–6.

4. Luo ZY, Wang SR, Liao YF, Zhou JS, Gu YL, Cen KF. Research on biomass fast pyrolysis for liquid fuel. Biomass Bioenerg. 2003;26:455–62.
5. Fjellerup J, Gjernes E, Hansen LK. Pyrolysis and combustion of pulverized wheat straw in a pressurized entrained flow reactor. Energy Fuels. 1996;10:649–51.
6. Dall'Ora M, Jensen PA, Jensen AD. Suspension combustion of wood: influence of pyrolysis conditions on char yield, morphology, and reactivity. Energy Fuels. 2008;22:2955–62.
7. Choct M. Enzymes for the feed industry: past, present and future. World Poultry Sci J. 2006;62:5–16.
8. Roberson KD. Use of dried distillers' grains with solubles in growing-finishing diets of Turkey hens. Int J Poultry Sci. 2003;2:389–93.
9. Nyachoti CM, House JD, Slominski BA, Seddon IR. Energy and nutrient digestibilities in wheat dried distillers' grains with solubles fed to growing pigs. J Sci Food Agr. 2005;85:2581–6.
10. Kleinschmit DH, Schingoethe DJ, Kalscheur KF, Hippen AR. Evaluation of various sources of corn dried distillers grains plus solubles for lactating dairy cattle. J Dairy Sci. 2006;89:4784–94.
11. Tavasoli A, Ahangari MG, Soni C, Dalai AK. Production of hydrogen and syngas via gasification of the corn and wheat dry distiller grains (DDGS) in a fixed-bed micro reactor. Fuel Process Technol. 2009;90:472–82.
12. Agler MT, Garcia ML, Lee ES, Angenent LT. Thermophilic anaerobic digestion to increase the net energy balance of corn grain ethanol. Environ Sci Technol. 2008;42:6723–9.
13. Kaparaju P, Serrano M, Angelidaki I. Optimization of biogas production from wheat straw stillage in UASB reactor. Appl Energ. 2010;87:3779–83.
14. Kumar A, Eskridge K, Jones DD, Milford AH. Steam–air fluidized bed gasification of distillers grains: Effects of steam to biomass ratio, equivalence ratio and gasification temperature. Bioresour Technol. 2009;100:2062–8.
15. Nowicki L, Antecka A, Bedyk T, Stolarek P, Stanisław Ledakowicz. The kinetics of gasification of char derived from sewage sludge. J Therm Anal Calorim. 2011;104:693–700.
16. Ghaly A, Ergüdenler A. Determination of the kinetic of barley straw using thermogravimetric analysis. Appl Biochem Biotechnol. 1994;45–46:35–50.
17. Miranda T, Esteban A, Rojas S, Montero I, Ruiz A. Combustion analysis of different olive residues. Int J Mol Sci. 2008;9:512–25.
18. Cordero T, Rodriguez-maroto JM, Rodriguez JJ. Kinetics of thermal decomposition of wood and wood components. Thermochim Acta. 1990;164:135–44.
19. Conesa JA, Caballero J, Marcilla A, Font R. Analysis of different kinetic models in the dynamic pyrolysis of cellulose. Thermochim Acta. 1995;254:175–92.
20. Blasi CD, Branca C, Errico GD. Degradation characteristics of straw and washed straw. Thermochim Acta. 2000;364:133–42.
21. Lapuerta M, Hernández JJ, Rodríguez J. Kinetics of devolatilisation of forestry wastes from thermogravimetric analysis. Biomass Bioenerg. 2004;27:385–91.
22. Maiti S, Purakayastha S, Ghosh B. Thermal characterization of mustard straw and stalk in nitrogen at different heating rates. Fuel. 2007;86:1513–8.
23. Valérie L, Dominique C, Eric L, Jean-Louis R. Kinetic study of forest fuels by TGA: Model-free kinetic approach for the prediction of phenomena. Thermochim Acta. 2010;497:1–6.
24. Flynn JH. The Temperature Integral—its use and abuse. Thermochim Acta. 1997;300:83–92.
25. Coats AW, Redrern JP. Kinetic parameters from thermogravimetric data. Nature. 1964;201:68–9.
26. Adanez J, Dediego RF. Reactivity of lignite chars withCO_2: influenee of the mine matter. Int Chem Eng. 1993;33:656–62.
27. Szekely J, Evans JW. A structural model for gas-solid reactions with a moving boundary. Chem Eng Sci. 1970;25:1091–107.
28. Shafizadeh F, DeGroot W F. Thermal Uses and Properties of Carbohydrates and Lignins. New York: Academic press INC; 1976.
29. Ivan M, Vahur O, Eric MS. Kinetics of the pyrolysis and combustion of olive oil solid waste. Ind Eng Chem Res. 1996;35:653–62.
30. Jauhiainen J, Conesa JA, Font R, Mart′ın-Gullón I. Kinetic modeling of biomass pyrolysis. J Anal Appl Pyrol. 2004;72:9–15.
31. Varhegyi G, Antal MJ, Jakab E, Szabo P. Pyrolysis behavior and kinetics of biomass derived materials. J Anal Appl Pyrol. 1997;42:73–87.
32. Fisher T, Hajaligol M, Waymack B, Kellogg D. Pyrolysis characteristics and kinetics of biomass residuals mixtures with lignite. J Anal Appl Pyrol. 2002;62:331–49.
33. Vamvuka D, Kakaras E, Kastanaki E, Grammelis P. Thermogravimetric analysis and devolatilization kinetics of wood. Fuel. 2003;82:1949–60.
34. Seebauer V, Petek J, Staudinger G. Effects of particle size, heating rate and pressure on measurement of pyrolysis kinetics by thermogravimetric analysis. Fuel. 1997;76:1277–82.
35. Senneca O. Kinetics of pyrolysis, combustion and gasification of three biomass fuels. Fuel Process Technol. 2007;88:87–97.
36. Arendt P, Van Heek K. Comparative investigations of coal pyrolysis under inert gas and H_2 at low and high heating rates and pressures up to 10 Mpa. Fuel. 1981;60:779.
37. Franco C, Pinto F, Gulyurtlu I, Cabrita I. The study of reactions influencing the biomass steam gasification process. Fuel. 2003;82:835–42.
38. Dupont C, Boissonnet G, Seiler J-M, Gauthier P, Schweich D. Study about the kinetic processes of biomass steam gasification. Fuel. 2007;86:32–40.
39. Sakaguchi M, Watkinson AP, Ellis N. Steam gasification of bio-oil and bio-oil/char slurry in a fluidized bed reactor. Energy Fuels. 2010;24:5181–9.